Ryanodine receptor leak mediated by caspase-8 activation leads to left ventricular injury after myocardial ischemia-reperfusion

Jérémy Fauconnier[a,b], Albano C. Meli[c], Jérôme Thireau[a,b], Stephanie Roberge[a,b], Jian Shan[c], Yassine Sassi[d], Steven R. Reiken[c], Jean-Michel Rauzier[a,b], Alexandre Marchand[d], David Chauvier[e], Cécile Cassan[a], Christine Crozier[a], Patrice Bideaux[a], Anne-Marie Lompré[d], Etienne Jacotot[e,f,g], Andrew R. Marks[c], and Alain Lacampagne[a,b,1]

[a]Institut de la Santé et de la Recherche Médicale, U1046, F-34295 Montpellier, France; [b]Universités Montpellier 1 and 2, Unité de Formation et de Recherche de Médecine, F-34295 Montpellier, France; [c]Russ Berrie Medical Science Pavilion, Columbia University College of Physicians & Surgeons, New York, NY 10032; [d]Institut de la Santé et de la Recherche Médicale/Université Pierre et Marie Curie Unité Mixte de Recherche S 956, Centre Hospitalier La Pitié-Salpétrière 91, 75634 Paris, France; [e]Theraptosis R&D Laboratories, Theraptosis S.A., F-93230 Romainville, France; [f]Institut de la Santé et de la Recherche Médicale U676, Hôpital Robert Debré, F-75019 Paris, France; and [g]Faculté de Médecine Denis Diderot, Université Paris 7, F-75019 Paris, France

Edited by Eric N. Olson, University of Texas Southwestern, Dallas, TX, and approved June 21, 2011 (received for review January 10, 2011)

Myocardial ischemic disease is the major cause of death worldwide. After myocardial infarction, reperfusion of infracted heart has been an important objective of strategies to improve outcomes. However, cardiac ischemia/reperfusion (I/R) is characterized by inflammation, arrhythmias, cardiomyocyte damage, and, at the cellular level, disturbance in Ca^{2+} and redox homeostasis. In this study, we sought to determine how acute inflammatory response contributes to reperfusion injury and Ca^{2+} homeostasis disturbance after acute ischemia. Using a rat model of I/R, we show that circulating levels of TNF-α and cardiac caspase-8 activity were increased within 6 h of reperfusion, leading to myocardial nitric oxide and mitochondrial ROS production. At 1 and 15 d after reperfusion, caspase-8 activation resulted in S-nitrosylation of the RyR2 and depletion of calstabin2 from the RyR2 complex, resulting in diastolic sarcoplasmic reticulum (SR) Ca^{2+} leak. Pharmacological inhibition of caspase-8 before reperfusion with Q-LETD-OPh or prevention of calstabin2 depletion from the RyR2 complex with the Ca^{2+} channel stabilizer S107 ("rycal") inhibited the SR Ca^{2+} leak, reduced ventricular arrhythmias, infarct size, and left ventricular remodeling after 15 d of reperfusion. TNF-α–induced caspase-8 activation leads to leaky RyR2 channels that contribute to myocardial remodeling after I/R. Thus, early prevention of SR Ca^{2+} leak trough normalization of RyR2 function is cardioprotective.

Myocardial infarction is, in the United States with >1.5 million new cases diagnosed each year, a leading cause of death. Reperfusion of infracted heart has been the main strategy to improve outcomes (1). However, cardiac ischemia/reperfusion (I/R) is characterized by arrhythmias, cardiomyocyte damage, inflammation, and, at the cellular level, disturbance in Ca^{2+} and redox homeostasis.

Elevated plasma levels of tumor necrosis factor α (TNF-α) have been reported in cardiac reperfusion injury, myocardial infarction, and in congestive heart failure. TNF-α induces pleiotropic effects that are mediated through activation of two distinct receptors: TNF receptor 1 (TNFR1) and TNF receptor 2 (TNFR2) (2). Most of the deleterious effects are mediated by TNFR1 signaling (3). TNF-α also has long-term beneficial effects due to the induction of cytoprotective genes involved in cellular growth, survival, and proliferation (4). Thus, release of TNF-α after myocardial injury may activate signaling pathways that promote either cardiac adaptation/protection or maladaptive responses. Multicenter trials using TNF-α antagonists in moderate to severe heart failure (HF) demonstrated adverse effects instead of benefits (5, 6). Therefore, a new therapeutic strategy specifically targeting early deleterious effects of TNF-α, without affecting its cytoprotective activity, remains of interest.

One of the early events in the TNF-α/TNFR1 signaling pathways is activation of caspase-8 (7). This pathway is initiated by recruitment of the adaptor protein Fas-associated via a death domain (FADD), which then recruits procaspase-8 into the death-inducing signaling complex (DISC). Caspase-8 activation leads to the generation of ceramide, mitochondrial reactive oxygen species (ROS) production, Bid cleavage, followed by cytochrome *c* release from mitochondria, and apoptosome formation, ultimately leading to activation of effectors caspases (i.e., caspase-3) and cell death (8–10). In parallel, acute nitric oxide (NO) production through activation of the endothelial nitric oxide synthase (eNOS), or increased expression of inducible nitric oxide synthase (iNOS) inhibit key apoptogenic signals triggered by TNF-α such as ceramide formation and caspase-8 (11, 12).

Increased ROS and/or NO-derived reactive species (RNS) change the redox environment of Ca^{2+} transporters and channels and, thus, affect cellular Ca^{2+} cycling (13). The cardiac ryanodine receptor (RyR2) that mediates sarcoplasmic reticulum (SR) Ca^{2+} release during excitation-contraction coupling contains ≈33 free thiol residues, rendering it highly sensitive to the cellular redox state. Cysteine oxidation facilitates RyR opening and SR Ca^{2+} leak (14, 15). Moreover, we have recently shown that S-nitrosylation of RyR1 (skeletal muscle) and RyR2 (cardiac muscle) and dissociation of their stabilizing subunit calstabin1 (FKBP12) or calstabin2 (FKBP12.6), respectively, induces SR Ca^{2+} leak, cardiac arrhythmia, skeletal muscle weakness, and remodeling in a Duchene muscular dystrophy (*mdx*) mouse model (16, 17).

In this study, we sought to determine whether TNF-α–induced caspase-8 activation would affect RyR2 S-nitrosylation leading to diastolic SR Ca^{2+} leak and left ventricular remodeling in a rat model of I/R. Using broad-spectrum caspase inhibitors and preferential caspase-8 inhibitors, and stabilization of the RyR2 macromolecular complex with a rycal (S107), we showed that early caspase-8 activation increases mitochondrial ROS and NO production, resulting in S-nitrosylation of RyR2 and depletion of calstabin2 from the channel complex causing a diastolic SR Ca^{2+} leak that leads to acute pathological left ventricular remodeling.

Author contributions: J.F., A.-M.L., E.J., A.R.M., and A.L. designed research; J.F., A.C.M., J.T., S.R., J.S., Y.S., S.R.R., J.-M.R., A.M., D.C., C. Cassan, C. Crozier, P.B., A.-M.L., E.J., and A.L. performed research; D.C., E.J., A.R.M., and A.L. contributed new reagents/analytic tools; J.F., A.C.M., J.T., S.R., Y.S., S.R.R., J.-M.R., A.M., D.C., C. Cassan, C. Crozier, P.B., A.-M.L., E.J., and A.L. analyzed data; and J.F., E.J., A.R.M., and A.L. wrote the paper.

Conflict of interest statement: A.R.M. is on the scientific advisory board and own shares in ARMGO Pharma, Inc., a start-up company developing RyR targeted drugs for clinical use in the treatment of heart failure and sudden death.

This article is a PNAS Direct Submission.

[1]To whom correspondence should be addressed. E-mail: alain.lacampagne@inserm.fr.

This article contains supporting information online at www.pnas.org/lookup/suppl/doi:10.1073/pnas.1100286108/-/DCSupplemental.

Results

Effect of TNF-α and Caspase-8 Activation on RyR2 Function in Vitro. Acute application of TNF-α (1 h, 10 ng/mL) to freshly isolated control cardiomyocytes induced caspase-8 like and caspase-3 like activities sequentially (Fig. S1*A*). In addition, application of TNF-α resulted in a progressive and significant increase in the Mitosox Red fluorescence within 1 h in control cells or in myocytes preincubated with a preferential caspase-3/7 inhibitor (Z-DEVD-FMK; 10 μM) (103 ± 10%, n = 30 and 90.5 ± 12%, n = 29, respectively), whereas there was no change in fluorescence in cells preincubated either with preferential caspase-8 inhibitors [Q-LETD-OPh (18), 10 μM; or Z-IETD-FMK, 10 μM] or with broad spectrum caspase inhibitor (Q-VD-OPh; 10 μM) (Fig. 1 *A* and *B*). Of note, this mitochondrial ROS production was associated with a significant $\Delta\Psi_m$ depolarization that was inhibited by caspase-8 inhibitors (Fig. S1*B*). Several studies have reported that TNF-α increases NO production either acutely through ceramide production and eNOS activation (12) or after induction of iNOS expression (19). Thus, we tested the effect of TNF-α on NO production by using DAF-FM, which increases its fluorescence when oxidized by NO (20). TNF-α application caused a progressive increase in the DAF-FM fluorescence, which was inhibited by caspase-8 inhibitor (32 ± 5%, n = 20 vs. 0.2 ± 0.8% n = 20; $P < 0.05$, Fig. 1 *C* and *D*). TNF-α-induced NO production was also significantly decreased in the presence of a ceramide catabolism inhibitor (NOE; 10 μM), suggesting that caspase-8–induced ceramide production is essential for TNF-induced NO production. Moreover, TNF-α failed to increase NO level when eNOS was inhibited (L-NIO; 1 μM) (Fig. 1*D*). These results suggest that TNF-α induced caspase-8 activation is an upstream event in the signaling pathways involving ceramide production (21) and eNOS activation (12).

Under these proinflammatory conditions, simultaneous production of superoxide anion ($O_2^{\cdot -}$) and NO can generate peroxynitrite formation (22). Among proteins involved in excitation-contraction coupling, RyR2 is highly sensitive to peroxynitrite and subsequent S-nitrosylation (13). In the present study, acute incubation of cardiomyocytes with TNF-α (10 ng/mL) for 1 h was sufficient to cause RyR2 S-nitrosylation and calstabin2 depletion from RyR2 complexes (Fig. 1*E*). TNF-α also increases open probability (Po) of RyR2 channels incorporated into planar lipid bilayers (Fig. 1*F*) and Ca^{2+}-spark frequency in intact ventricular cardiomyocytes (Fig. 1*G*). In the presence of the caspase-8 inhibitor, Q-LETD-OPh, the TNF-α–induced changes in RyR2

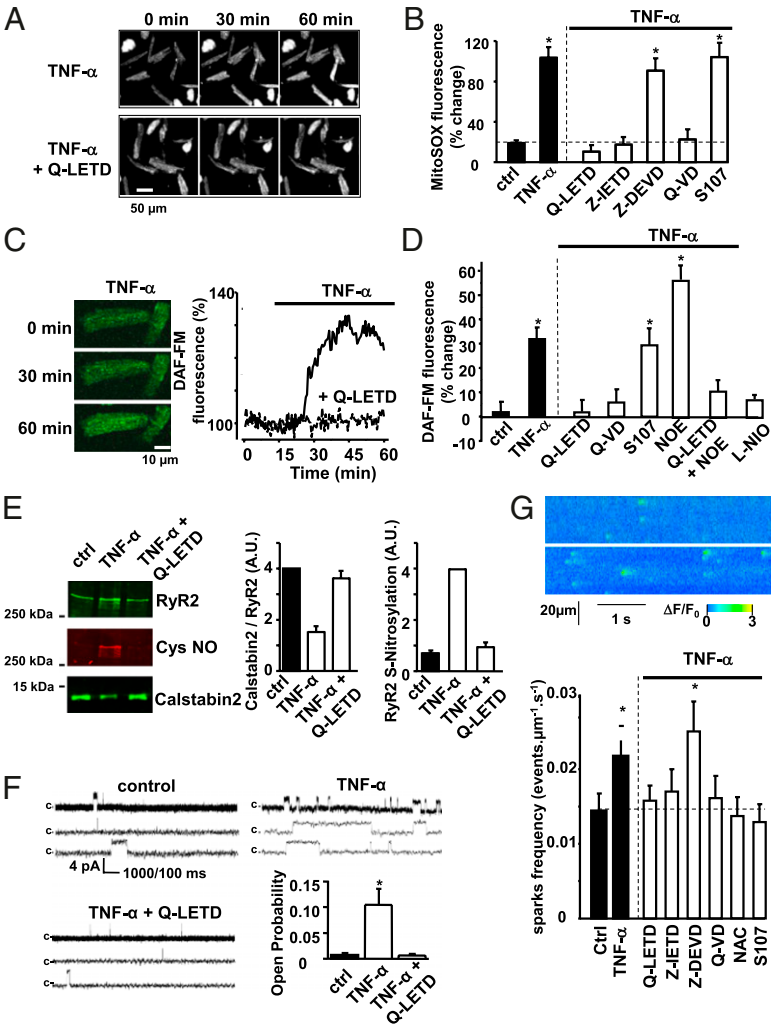

Fig. 1. (*A*) Representative MitoSOX red fluorescence recorded at 0, 30, and 60 min of TNF-α (10 ng/mL) or TNF-α + Q-LETD-OPh (10 μM) application in single ventricular rat cardiomyocytes. (*B*) Mean data ± SEM of normalized MitoSOX red fluorescence after 60 min of TNF-α application. *, statistical difference compared with control conditions ($P < 0.05$; $n \geq 20$ cells in each conditions). Each caspase inhibitor (10 μM) was preincubated 15 min before TNF-α application. For S107 experiments, the animals were orally treated with S107 (25 mg/100 mL, in drinking water) 1 wk before cells isolation. Note that caspase-8 inhibitors (Q-LETD-OPh and Z-IETD-FMK) and broad spectrum caspase inhibitor (Q-VD-OPh) prevents TNF-α–induced mitochondrial ROS production, whereas caspase-3/7 inhibitor (Z-DEVD-FMK) and S107 did not. (*C Left*) Typical images of TNF-α–induced NO production measured with DAF-FM using confocal microscope. (*C Right*) Time change of normalized DAF-FM fluorescence in presence of TNF-α (10 ng/mL) or TNF-α + Q-LETD-OPh (10 μM). (*D*) Mean data ± SEM of normalized DAF-FM fluorescence after 60 min of TNF-α application. *, statistical difference compared with control conditions ($P < 0.05$; $n \geq 20$ cells in each conditions). Note that caspase-8 inhibitor (Q-LETD-OPh), broad spectrum caspase inhibitor (Q-VD-OPh), and eNOS inhibitor (L-NIO) prevent TNF-α–induced NO production, whereas ceramidase inhibitor (NOE) or S107 did not. (*E*) Representative cardiac RyR2 immunoprecipitation and immunoblots and bar graphs showing Cys nitrosylation of cardiac RyR2 and the amount of calstabin2 in the cardiac RyR2 complex. Bar graph shows the relative amount of calstabin2 associated with the RyR2 channel complex for each group determined by dividing the calstabin2 signals by the total amount of RyR2 that was immunoprecipitated (a.u.). The bar graphs, depicting the relative amount of RyR2 S-nitrosylation for each group, were determined by dividing the Cys-NO signals by the total amount of RyR2 immunoprecipitated (a.u.). Data presented as mean ± SEM (*F*) RyR2 single channels isolated from left ventricular cardiomyocytes treated 1 h with TNF-α (10 ng/mL), or with Q-LETD-OPh (10 μM) followed by 1 h with TNF-α (10 ng/mL). (*F*) Representative RyR2 single-channel traces from control, TNF-α treated, and Q-LETD-OPh+TNF-α–treated samples. Single channel activities were recorded at 150 nmol/L free cytosolic (*cis*) Ca^{2+} concentration and 53 mM $Ca(OH)_2$ luminal (*trans*) at 0 mV. Channel openings are shown as upward deflections from the closed level (c-). Example of channel activity is shown at two different time scales (10 s for one upper trace and 1 s for two lower traces in each block) as indicated by dimension bars. Summary data of relative values of RyR2 Po of control, TNF-α treated and Q-LETD-OPh+TNF-α treated samples. *$P < 0.05$ vs. control. (*G*) Spontaneous SR Ca^{2+} release events were recorded in fluo-4-AM–loaded intact cardiomyocytes by laser scanning confocal microscopy. Representative $\Delta F/F$ lines can images (1.54 ms per line) were recorded in the absence of (control) or after 1 h of TNF-α incubation. Ca^{2+} sparks frequency is used as an index of diastolic SR Ca^{2+} leak. Caspases inhibitors are indicated as follows: Q-LETD, Q-LETD-OPh; Z-IETD, Z-IETD-FMK; Z-DEVD, Z-DEVD-FMK; Q-VD, Q-VD-OPh. Data are expressed as mean ± SEM, (*$P < 0.05$ vs. control; $n \geq 30$ cells in each condition).

S-nitrosylation, calstabin2 binding to the RyR2 complex, RyR2 Po, and Ca^{2+} sparks frequency were prevented (Fig. 1 *E–G*). Of note, RyR2 PKA-dependent phosphorylation site (ser2808) was unchanged (Fig. S2). The increase in Ca^{2+} sparks frequency was also prevented by the RyR Ca^{2+} release channel stabilizer "rycal" S107 (Fig. 1*G*). Q-LETD-OPh or S107 did not change basal Ca^{2+} sparks frequency, and a combined treatment similarly decreased TNF-α–increased sparks frequency compared with a single treatment with Q-LETD-OPh or S107 (Fig. S1*C*). However, S107 treatment did not prevent $\Delta\Psi_m$ depolarization (Fig. S1*B*), mitochondrial ROS production (Fig. 1 *A* and *B*), or NO production (Fig. 1 *C* and *D*), suggesting that RyR2 leak does not affect caspase-8–mediated mitochondrial dysfunction. The antioxidant *N*-acetyl cysteine (NAC) also normalized Ca^{2+} spark frequency (Fig. 1*G*). Moreover, TNF-α decreased the Ca^{2+} transient amplitude, Ca^{2+} release kinetics, SR Ca^{2+} load, and cell shortening (Fig. S3). Q-LETD-OPh prevented the TNF-α–induced decrease in the Ca^{2+} transient amplitude, Ca^{2+} release kinetics, SR Ca^{2+} load, and cell shortening (Fig. S3). S107 or NAC did not affect basal Ca^{2+} transient characteristics (Fig. S3 *B–E*). In such conditions and in agreement with a previous report (2), TNF-α induced positive effects on Ca^{2+} handling and cell shortening (Fig. S3 *B–E*). Thus, TNF-α–mediated ROS/NO production via caspase-8 activation increased RyR2 S-nitrosylation and SR Ca^{2+} leak.

Roles of Caspase-8 and RyR2 Leak in Myocardial Reperfusion Injury. To determine whether the TNF-α–induced SR Ca^{2+} leak via RyR2 channels contributes to reperfusion injury, we performed 30 min of ischemia followed by reperfusion in vivo in rats. TNF-α plasma levels were detected at 1 h and returned to baseline 6 h after reperfusion (276 ± 48 pg/mL at 1 h, $n = 6$; Fig. 2*A*). In parallel, cardiac caspase-8 activity was also significantly increased by 1 h after reperfusion, peaked at 6 h, and returned to baseline by 24 h (Fig. 2*B*). In addition, Bid cleavage increased significantly after 24 h of reperfusion as shown by the increase level of the truncated Bid isoform (Fig. S4). RyR2 S-nitrosylation and calstabin2 depletion were also observed 24 h after reperfusion (Fig. 2*C*) without any change in phosphorylation of RyR2 at ser2808 (Fig. S2). S107 (25 mg/100 mL, in drinking water) treatment for 1 wk before surgery prevented calstabin2 depletion from the RyR2 complex but did not affect S-nitrosylation of the channel (Fig. 2*C*). In contrast, Q-LETD-OPh treatment (1 mg/kg i.p.) 15 min before reperfusion inhibited both RyR2 S-nitrosylation and depletion of calstabin2 from the RyR2 complex (Fig. 2*C*). In addition, both S107 and Q-LETD-OPh significantly reduced myocardial infarct size [infarct area/area at risk (IA/AAR)] compared with DMSO-treated rats (Fig. 2*D*). Similar experiments were performed with an anti-TNF-α (Etanercept) treatment before surgery. As with S107 or Q-LETD-OPh, Etanercept reduced infarct size by ≈50% (Fig. S5). The severity of the ischemic insult was similar in the different groups, as shown by the ratios of AAR relative to ventricle area (V) (AAR/V= 39 ± 8% in DMSO treated, $n = 10$; 35 ± 6% in Q-LETD-OPh treated, $n = 8$; 38 ± 6% in S107 treated, $n = 5$; 39 ± 7% in Etanercept treated). Moreover, on calstabin2 KO mice, myocardial infarct size was significantly increased compared with WT mice and S107 was inefficient, whereas it reduced significantly infarct size in WT (Fig. S6*A*). Similarly, RyR2 S-nitrosylation was increased in calstabin2 KO after I/R (Fig. S6*B*). Altogether these results corroborate in vivo the role of TNF-α in caspase-8/RyR2-mediated reperfusion injury.

SR Ca^{2+} leak is thought to play a role in triggering arrhythmias during the early phase of reperfusion (23, 24). We observed numerous ventricular extrasystoles and sustained ventricular tachycardia during the first 12 h of reperfusion (Fig. S7 *A–E*). Q-LETD-OPh and S107 treatment both significantly reduced arrhythmias (Fig. S7*A* and *C–E*). In WT mice injected with TNF-α, we measured Bid cleavage, RyR2 S-nitrosylation, calstabin2 dissociation, and ventricular arrhythmias (Figs. S7*F* and S8). As for I/R, TNF-α in vivo significantly increased ventricular extrasystoles, Bid cleavage, RyR2 S-nitrosylation, and calstabin2 dissociation. All these effects were prevented by caspase-8 inhibition (Figs. S7*F* and S8). Thus, inhibition of caspase-8 and prevention of calstabin2 depletion from the RyR2 complex with S107 prevents early reperfusion injury and associated arrhythmias.

Role of Caspase-8 and RyR2 Leak in Left Ventricular Remodeling. We subsequently analyzed and compared the longer-term effects of either early caspase-8 inhibition or S107 treatment on left ventricular remodeling 15 d after myocardial reperfusion. Histological analyses of the left ventricle were performed by using Masson trichrome staining to detect collagen fibers. There was an increase in extracellular matrix (i.e., fibrosis) that was prevented when animals were treated with Q-LETD-OPh (1 mg/kg i.p.), 15 min before the reperfusion or pretreated with S107 (25 mg/100 mL in the drinking water) 1 wk before ischemia and up to 72 h after reperfusion, compared with vehicle-treated animals (Fig. 3*A*). As an index of hypertrophy, HW/BW ratio was sig-

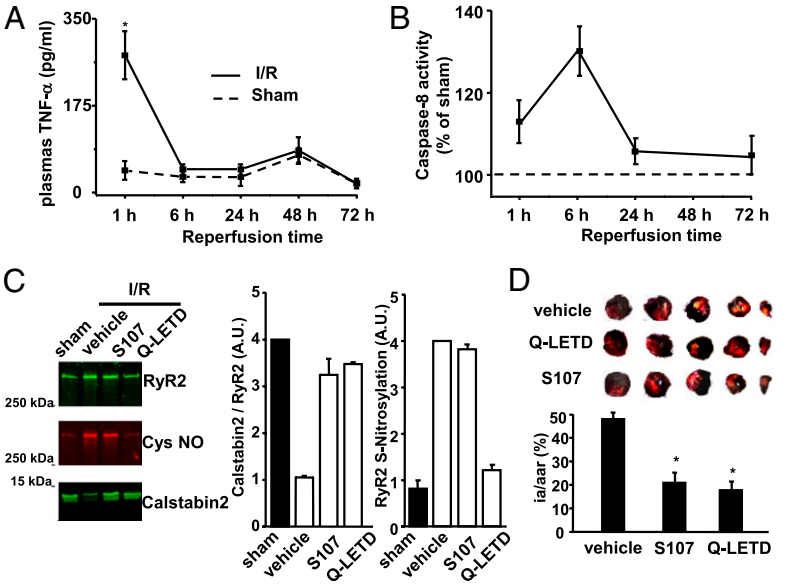

Fig. 2. (*A*) Circulating levels of TNF-α after reperfusion compared with sham-operated animals. Plasma level of TNF-α was maximal after 1 h of reperfusion and returned to normal values within 6 h of reperfusion. (*$P < 0.05$ vs. sham; $n \geq 6$ animal in each conditions). (*B*) Normalized caspase-8 activity measured in left ventricular free wall homogenates after different time of reperfusion. Increased caspase-8 activity was maximal after 6 h of reperfusion and return to normal values within the first 24 h of reperfusion. ($n = 6$ animals). (*C*) Representative cardiac RyR2 immunoprecipitation and immunoblots and bar graphs showing Cys nitrosylation of cardiac RyR2 and depletion of calstabin2 from the cardiac RyR2 complex, 24 h after reperfusion in a rat model of ischemia-reperfusion (I/R) treated either with the vehicle (DMSO, i.p. injected), S107 (drinking water; 25 mg/100 mL), or Q-LETD-OPh (i.p. injected 15 min before reperfusion). The relative amount of calstabin2 associated with the channel complex was determined by dividing the calstabin2 signals by the total amount of RyR2 immunoprecipitated (a.u.). The relative amount of RyR2 S-nitrosylation for each group was determined by dividing the Cys-NO signals by the total amount of RyR2 immunoprecipitated (a.u.). Data presented as mean ± SEM. (*D*) Representative sections of TTC-stained hearts. Quantification was done by normalizing the infarct area (IA) to the area at risk (AAR). Treatment with Q-LETD-OPh or S107 reduces infarct size after 24 h of reperfusion. (*$P < 0.05$ vs. sham; $n \geq 6$ animals in each conditions). Caspase-8 inhibitor, Q-LETD-OPh, is indicated as Q-LETD.

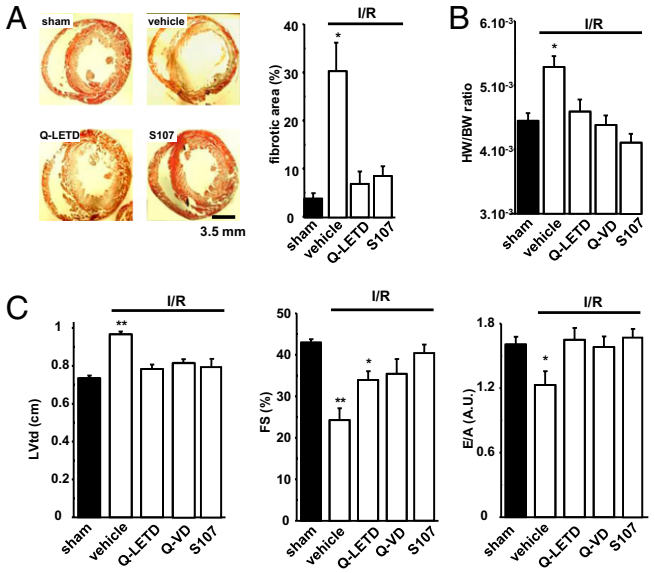

Fig. 3. Left ventricular remodeling 15 d after reperfusion. (*A*) Heart section stained with Masson trichrome revealed a major increase in fibrosis that was prevented when animals were i.p. injected in Q-LETD-OPh, 15 min before the reperfusion or when pretreated with S107 (1 wk before ischemia and up to 72 h after reperfusion) compared with vehicle treated animals. (*$P < 0.05$ vs. sham; $n \geq 6$ animals in each conditions). (*B*) Heart weight to body weight ratio was significantly increased in DMSO-treated animals and unchanged in Q-LETD-OPh- or S107-treated animals (*$P < 0.05$ vs. sham; $n \geq 10$ animals in each conditions). (*C*) Echocardiographic parameters analyzed 15 d after reperfusion. Left ventricular telediastolic diameter (LVtd; *Left*), fractional shortening (FS; *Center*) and E wave over A wave ratio (E/A; *Right*) are significantly affected in DMSO-treated animal. Echocardiographic parameters were significantly enhanced when animals where i.p. injected in Q-LETD-OPh or with S107. (*$P < 0.05$ vs. sham; $n \geq 8$ animals in each conditions). Caspases inhibitors are indicated as follows: Q-LETD, Q-LETD-OPh; Q-VD, Q-VD-OPh.

nificantly increased in DMSO-treated animals and unchanged in Q-LETD-OPh or S107-treated animals (Fig. 3*B*). After I/R, the rats exhibited evidence of cardiac dysfunction with an increase in LVtd and a decrease in fractional shortening (Fig. 3*C*), both of which were significantly improved in animals treated with Q-LETD-OPh or S107 (Fig. 3*C*).

The cardiac ventricular remodeling observed 2 wk after reperfusion was associated with RyR2 S-nitrosylation, calstabin2 depletion from the RyR2 complex, without any modification of RyR2 phosphorylation at ser2808 (Fig. 4*A* and Fig. S2), and with an increase in RyR2 channel Po measured under conditions corresponding to diastole (low activating $[Ca^{2+}] \approx 150$ nM; Fig. 4*B*). These results are consistent with a diastolic SR Ca^{2+} leak. Once again, S107 inhibited depletion of calstabin2 from the RyR2 complexes without affecting S-nitrosylation of RyR2, whereas Q-LETD-OPh normalized both. RyR2 channel PO, measured at 150 nM cytosolic Ca^{2+}, was partially or totally reduced to that observed in control channels from animals treated with S107 or Q-LETD-OPh, respectively. At the cellular level, Ca^{2+} transient amplitudes were decreased by ≈20% and the rising phases was significantly slower in vehicle-treated animals (Fig. S9 *A* and *B*). These changes were accompanied by decreased SR Ca^{2+} content and fractional cell shortening (Fig. S9 *C* and *D*). Thus, S107 or Q-LETD-OPh treatment prevented altered Ca^{2+} handling and impaired cell shortening.

Cytosolic Ca^{2+} regulates the nuclear translocation of some transcription factors and the expression of Ca^{2+}-dependent genes known to contribute to ventricular remodeling (25). In that context, we hypothesized that the diastolic SR Ca^{2+} leak via RyR2 channels after I/R might contribute to the cardiac remodeling process. The nuclear factor of activated T cells (NFAT) is a transcription factor involved in cardiac hypertrophy (26). Elevated cytosolic $[Ca^{2+}]_i$ activates the calmodulin-activated serine/threonine protein phosphatase calcineurin, which dephosphorylates NFATc resulting in nuclear translocation of NFAT and activation of hypertrophy genes (27) and immunologically important genes, such as TNF-α (28). We examined cytosolic to nuclear translocation of NFAT and observed increased NFAT after I/R (Fig. 4*C*). When the animals were treated with caspase-8 inhibitor (Q-LETD-OPh) or rycal (S107), NFAT was retained in the cytosol at levels similar to those observed in sham-operated animals and may contribute to the reduction in hypertrophy shown in Fig. 3*B*. Additionally, mRNA levels of the heart failure marker ANF were also significantly reduced with both treatments (Fig. 4*D*). In addition to lower levels of collagen (Fig. 3*A*), interstitial fibrosis as evidenced by increased levels of fibronectin mRNA was also prevented by caspase-8 inhibition or S107 inhibition of SR Ca^{2+} leak (Fig. 4*D*). I/R also increased mRNA levels of molecules involved in TNF-α signaling including TNFR1, TNFR2, caspase-8, and TNF-α (Fig. 4*E*). This increase in mRNA levels was prevented by the caspase-8 inhibitor (Q-LETD-OPh) and by S107, suggesting a reduced inflammatory response. Taken together, these results indicate that an increase in ROS and NO production, via early caspase-8 activation, induces RyR2 S-nitrosylation and diastolic SR Ca^{2+} leak, which contribute to I/R injury and long-term left ventricular remodeling.

Discussion

The therapeutic strategy of rapid reperfusion of ischemic myocardium is designed to preserve cardiac function. However, reperfusion itself has notable adverse effects including arrhythmias and cell death (29, 30). We now show that inhibiting RyR2 mediated diastolic SR Ca^{2+} leak with a unique orally available drug called rycal (S107), which stabilizes the channel, or by caspase-8 inhibition, significantly reduces reperfusion injury, infarct extension, and left ventricular remodeling in the later phase of reperfusion (i.e., 15 d after reperfusion). LV remodeling after ischemia is caused by multiple factors including: (*i*) myocardial cell death; (*ii*) ROS production and inflammatory cytokines; (*iii*) structural changes of myocardium in response to mechanical stress; and (*iv*) myocardial fibrosis (31, 32). The present study reports the unique finding that inhibition of RyR2 mediated diastolic SR Ca^{2+} leak before the reperfusion is sufficient to substantially reduce reperfusion injury, myocardial cell death, fibrosis, left ventricular remodeling, and inflammation.

In this study, we present a unique TNF-α–mediated signaling pathway wherein caspase-8 activation leads to S-nitrosylation of RyR2 and calstabin2 depletion from the channel complex. The subsequent increase in diastolic SR Ca^{2+} leak contributes to reperfusion injury and left ventricular remodeling after acute I/R. TNFR1 is a death receptor that activates initiator caspases including caspase-8 (8). The resulting activation of caspase-8 is either sufficient to trigger the proteolytic activation of other caspases (i.e., caspase-3), or requires the proteolytic activation of proapoptotic proteins of the Bcl2 family in particular Bid, which triggers a loss of mitochondrial inner membrane potential $\Delta\psi m$ and ROS generation (10, 33–35). In cardiomyocytes, caspase-8 inhibition prevented TNF-α–induced loss of $\Delta\psi m$ and mitochondrial release of cytochorme *c* (10). Alternatively, the TNF/TNFR1 complex is thought to regulate sphingolipid signaling pathways (36). After TNF-α binds to TNFR1 an early weak recruitment of FADD and stimulation of caspase-8 in the cell are sufficient to activate sphingomyelinase (21). Activation of sphingomyelinase initiates sphingolipid metabolism with ceramide, sphingosine, and sphingosine-1-phosphate formation and permits death-receptor oligomerization and caspase-8 activation (37). These bioactive phospholipids induce cellular responses, such as mitochondrial ROS production (38) and NO synthesis (39). Hence, early inhibition of caspase-8 prevents TNF-α induced mitochondrial dysfunction and NO production (10) (Fig. 1). Concomitant ROS production and NO production would affect cellular signaling most likely through peroxynitrite formation and S-nitrosylation (13, 22). Oxidation of thiols on RyR2 may activate the channels

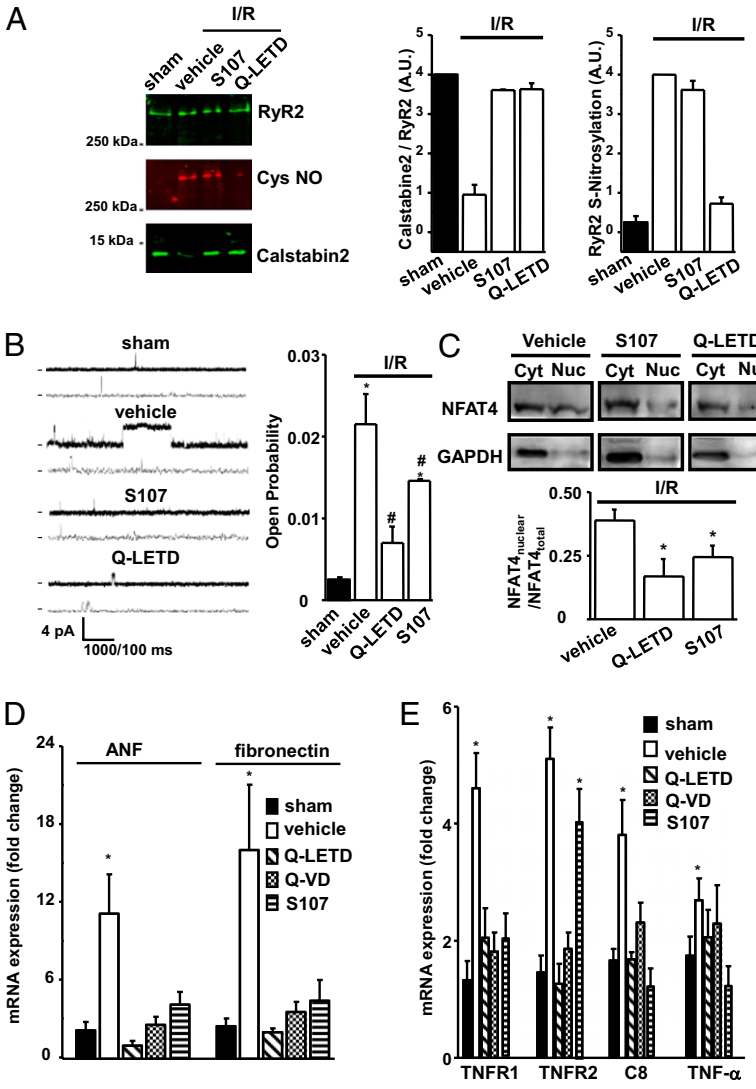

Fig. 4. (*A*) Representative cardiac RyR2 immunoprecipitation and immunoblots and bar graphs showing Cys nitrosylation and depletion of calstabin2 from the cardiac RyR2 complex, 2 wk after reperfusion. Levels of proteins in the RyR2 complex were normalized to the total amount of RyR2 (a.u.). Data presented as mean ± SEM. (*B*) RyR2 channels isolated from hearts 15 d after reperfusion. Representative single-channel traces recorded at 150 nmol/L free cytosolic (*cis*) Ca^{2+} concentration and 53 mM $Ba(OH)_2$ luminal (*trans*) at 0 mV. Channel openings are shown as upward deflections from the closed level (c-). Example of channel activity is shown at two different time scales (10 s for one upper trace and 1 s for two lower traces in each block) as indicated by dimension bars. Summary data of relative values of RyR2 normalized Po under different treatment conditions are indicated in the labeled legend. The single channel Po at 150 nmol/L free cytosolic Ca^{2+} concentration was normalized to the Po at 5,000 nmol/L free cytosolic Ca^{2+} concentration. *$P < 0.05$ vs. sham. #$P < 0.05$ vs. DMSO. Data are the means ± SE of 5–9 experiments for each group. (*C*) Western blot showing the presence of NFAT4 in cytosolic and nuclear fractions from different cardiac samples. The low level of GAPDH in the nuclear fraction indicates that these fractions were not contaminated by cytosol. The histograms represent the ratio of nuclear NFAT4 to cytosolic plus nuclear NFAT4. (*D*) mRNA expression level of Atrial Natriuretic Factor (ANF) and fibronectin in left ventricular free wall 15 d after reperfusion. (*$P < 0.05$ vs. sham; $n \geq 8$ animals in each conditions). (*E*) mRNA expression level of TNF-α signaling cascade key proteins such as TNF-α receptor 1 and 2 (TNFR1 and TNFR2), caspase-8 (C8), and TNF-α. Note that i.p. injection 15 min before reperfusion of Q-LETD-OPh or Q-VD-OPh or a pretreatment with S107 (1 wk before ischemia and up to 72 h after reperfusion) normalized mRNA expression level compared with DMSO-treated animals. (*$P < 0.05$ vs. sham; $n \geq 8$ animals in each conditions). Caspases inhibitors are indicated as follow: Q-LETD, Q-LETD-OPh; Q-VD, Q-VD-OPh.

resulting in a diastolic SR Ca^{2+} leak under pathological conditions (13, 15). Here, we show that S-nitrosylation and diastolic SR Ca^{2+} leak are associated with calstabin2 depletion from the channel complex, which is prevented by pharmacological inhibition of caspase-8 or with rycal S107 treatment. Of note, only caspase-8 inhibition prevented both calstabin2 depletion and S-nitrosylation. These results suggest that changes in the redox environment of the channel may lead to calstabin2 depletion and increased RyR2 channel activity under pathological conditions as shown in heart failure (15, 17).

SR Ca^{2+} leak is thought to trigger cellular damage after acute ischemia and reperfusion. Several studies have reported RyR2 dysfunction after I/R (24). Ca^{2+} overload has been reported to play a pathological role after reperfusion and ventricular arrhythmias (40, 41). Moreover, reperfusion is associated with the recovery of ATP phosphorylation potential, which restores SR Ca^{2+}-ATPase activity and increases Ca^{2+} sequestration into the SR (24). SR Ca^{2+} overload can cause oscillations of cytosolic Ca^{2+}. Short-term oscillations in cytosolic Ca^{2+} have been implicated in the genesis of reperfusion arrhythmias (23). Indeed, caspase-8 inhibition, which prevents early RyR2 dysfunction, has a profound impact on reperfusion arrhythmias (Fig. 2). In addition, these results suggest a connection between circulating TNF-α levels and arrhythmias in acute ischemia (42, 43).

During I/R, aberrant intracellular Ca^{2+} leak is taken up by the mitochondria (44). Ca^{2+} accumulation in the mitochondria leads to activation of mitochondrial permeability transition pore (MPTP) (45). Immediately after MPTP activation, mitochondria swell and release apoptogenic factors like cytochrome *c* and AIF, which activates caspase-dependent and independent execution of apoptosis. This study points out a potential involvement of a dual detection mechanisms sensitizing large-scale MPTP opening and mitochondrial membrane permeabilization (46–48). Accordingly, this sensitizing mechanism suggests that caspase-8–induced mitochondrial depolarization alone, without SR Ca^{2+} leak, will not be sufficient to trigger cell death but would require a commitment $[Ca^{2+}]_{mito}$ oscillations. Discrete modification of the SR Ca^{2+} leak may thus be sufficient to prevent large scale swelling and allowing functional recovery of the mitochondria (46–48). The present study suggests that leaky RyR2 may contribute to mitochondrial Ca^{2+} accumulation during I/R and to an amplification loop leading to reperfusion injury (9) given that inhibiting calstabin2 dissociation from the RyR2 complex reduces RyR2-mediated SR Ca^{2+} leak and is protective. Improving SR Ca^{2+} handling thus appears to be a potential unique target for reducing reperfusion injury, independently of reducing arrhythmia occurrence per se (24, 49).

In conclusion, the present study highlights the pathophysiological roles of TNF-α–induced caspase-8 activation and ROS/NO production, in the control of RyR2 function after acute myocardial infarction. Early reperfusion induced S-nitrosylation of RyR2 and calstabin2 depletion from the channel complex.

Caspase-8 activation also participates in reperfusion injury. Thus, both caspase-8 inhibition and RyR2/calstabin2 normalization are potential targets for the prevention of the effects of reperfusion, including myocardial cell death, arrhythmias, and late left ventricular remodeling after acute myocardial infarction.

Materials and Methods

See *SI Materials and Methods* for detailed descriptions.

Animal Model and Cell Dissociation. Eight-week-old Wistar Kyoto rats (Janvier) were used. The investigations conformed to the guidelines for the Care and Use of Laboratory Animals (National Institutes of Health No. 85–23, revised 1996) and European directives (96/609/EEC). For I/R protocol, the left coronary artery was ligated for 30 min (rats) and 1 h (mice). After 15 min of ligation, animals were randomly given vehicle (10% DMSO in 0.9% saline), Q-VD-OPh (i.p., 1 mg/kg in 10% DMSO), or Q-LETD-OPh (i.p., 1 mg/kg in 10% DMSO). In some experiments, animals were pretreated with S107 (25 mg/100 mL in the drinking water) 1 wk before ischemia and up to 72 h after reperfusion). Single cardiomyocytes were enzymatically isolated from the left ventricles as described before (50).

Statistics. Data are presented as mean ± SEM. Statistical significance was assessed by using the Student *t* test (for paired or unpaired samples) or when three or more groups were compared, one-way analysis of variance (ANOVA) with a Newman–Keuls post hoc test. $P < 0.05$ was considered significant.

ACKNOWLEDGMENTS. We thank C. Garraud-Moquereau, for technical assistance; N. Brunel, Plateforme Technologique Phénotypage du Petit Animal et Microdosages, IFR65/U515, Paris, for technical assistance with the TNF-α assay; and Prof. J. Morel, Montpellier Hospital, for providing Etanercept. This work was supported by the Institut de la Santé et de la Recherche Médicale, Région Languedoc Roussillon, and the Leducq Foundation, CAERUS Transatlantic Network of Excellence.

1. Piot C, et al. (2008) Effect of cyclosporine on reperfusion injury in acute myocardial infarction. *N Engl J Med* 359:473–481.
2. Defer N, Azroyan A, Pecker F, Pavoine C (2007) TNFR1 and TNFR2 signaling interplay in cardiac myocytes. *J Biol Chem* 282:35564–35573.
3. Torre-Amione G, et al. (1995) Expression and functional significance of tumor necrosis factor receptors in human myocardium. *Circulation* 92:1487–1493.
4. Sack MN, Smith RM, Opie LH (2000) Tumor necrosis factor in myocardial hypertrophy and ischaemia—an anti-apoptotic perspective. *Cardiovasc Res* 45:688–695.
5. Coletta AP, Clark AL, Banarjee P, Cleland JG (2002) Clinical trials update: RENEWAL (RENAISSANCE and RECOVER) and ATTACH. *Eur J Heart Fail* 4:559–561.
6. Mann DL, et al. (2004) Targeted anticytokine therapy in patients with chronic heart failure: Results of the Randomized Etanercept Worldwide Evaluation (RENEWAL). *Circulation* 109:1594–1602.
7. Ashkenazi A, Dixit VM (1998) Death receptors: Signaling and modulation. *Science* 281: 1305–1308.
8. Kroemer G, Galluzzi L, Brenner C (2007) Mitochondrial membrane permeabilization in cell death. *Physiol Rev* 87:99–163.
9. Luo X, Budihardjo I, Zou H, Slaughter C, Wang X (1998) Bid, a Bcl2 interacting protein, mediates cytochrome c release from mitochondria in response to activation of cell surface death receptors. *Cell* 94:481–490.
10. Zhu J, Liu M, Kennedy RH, Liu SJ (2006) TNF-alpha-induced impairment of mitochondrial integrity and apoptosis mediated by caspase-8 in adult ventricular myocytes. *Cytokine* 34:96–105.
11. Barsacchi R, et al. (2002) Cyclic GMP-dependent inhibition of acid sphingomyelinase by nitric oxide: An early step in protection against apoptosis. *Cell Death Differ* 9: 1248–1255.
12. Barsacchi R, et al. (2003) Activation of endothelial nitric-oxide synthase by tumor necrosis factor-alpha: A novel pathway involving sequential activation of neutral sphingomyelinase, phosphatidylinositol-3′ kinase, and Akt. *Mol Pharmacol* 63:886–895.
13. Zima AV, Blatter LA (2006) Redox regulation of cardiac calcium channels and transporters. *Cardiovasc Res* 71:310–321.
14. Xu L, Eu JP, Meissner G, Stamler JS (1998) Activation of the cardiac calcium release channel (ryanodine receptor) by poly-S-nitrosylation. *Science* 279:234–237.
15. Yano M, et al. (2005) Correction of defective interdomain interaction within ryanodine receptor by antioxidant is a new therapeutic strategy against heart failure. *Circulation* 112:3633–3643.
16. Bellinger AM, et al. (2009) Hypernitrosylated ryanodine receptor calcium release channels are leaky in dystrophic muscle. *Nat Med* 15:325–330.
17. Fauconnier J, et al. (2010) Leaky RyR2 trigger ventricular arrhythmias in Duchenne muscular dystrophy. *Proc Natl Acad Sci USA* 107:1559–1564.
18. Dzietko M, et al. (2008) A critical role for Fas/CD-95 dependent signaling pathways in the pathogenesis of hyperoxia-induced brain injury. *Ann Neurol* 64:664–673.
19. Maciejewski JP, et al. (1995) Nitric oxide suppression of human hematopoiesis in vitro. Contribution to inhibitory action of interferon-gamma and tumor necrosis factor-alpha. *J Clin Invest* 96:1085–1092.
20. Kojima H, et al. (1998) Detection and imaging of nitric oxide with novel fluorescent indicators: Diaminofluoresceins. *Anal Chem* 70:2446–2453.
21. Sawada M, et al. (2004) Molecular mechanisms of TNF-alpha-induced ceramide formation in human glioma cells: P53-mediated oxidant stress-dependent and -independent pathways. *Cell Death Differ* 11:997–1008.
22. Pacher P, Beckman JS, Liaudet L (2007) Nitric oxide and peroxynitrite in health and disease. *Physiol Rev* 87:315–424.
23. Lakatta EG, Guarnieri T (1993) Spontaneous myocardial calcium oscillations: Are they linked to ventricular fibrillation? *J Cardiovasc Electrophysiol* 4:473–489.
24. Zucchi R, Ronca F, Ronca-Testoni S (2001) Modulation of sarcoplasmic reticulum function: A new strategy in cardioprotection? *Pharmacol Ther* 89:47–65.
25. Passier R, et al. (2000) CaM kinase signaling induces cardiac hypertrophy and activates the MEF2 transcription factor in vivo. *J Clin Invest* 105:1395–1406.
26. Molkentin JD (2000) Calcineurin and beyond: Cardiac hypertrophic signaling. *Circ Res* 87:731–738.
27. Wilkins BJ, Molkentin JD (2004) Calcium-calcineurin signaling in the regulation of cardiac hypertrophy. *Biochem Biophys Res Commun* 322:1178–1191.
28. Rao A, Luo C, Hogan PG (1997) Transcription factors of the NFAT family: Regulation and function. *Annu Rev Immunol* 15:707–747.
29. Buja LM (2005) Myocardial ischemia and reperfusion injury. *Cardiovasc Pathol* 14: 170–175.
30. Yellon DM, Hausenloy DJ (2007) Myocardial reperfusion injury. *N Engl J Med* 357: 1121–1135.
31. Hori M, Nishida K (2009) Oxidative stress and left ventricular remodelling after myocardial infarction. *Cardiovasc Res* 81:457–464.
32. Peng J, Gurantz D, Tran V, Cowling RT, Greenberg BH (2002) Tumor necrosis factor-alpha-induced AT1 receptor upregulation enhances angiotensin II-mediated cardiac fibroblast responses that favor fibrosis. *Circ Res* 91:1119–1126.
33. Peter ME, Krammer PH (2003) The CD95(APO-1/Fas) DISC and beyond. *Cell Death Differ* 10:26–35.
34. Scaffidi C, et al. (1998) Two CD95 (APO-1/Fas) signaling pathways. *EMBO J* 17: 1675–1687.
35. Schulze-Osthoff K, et al. (1992) Cytotoxic activity of tumor necrosis factor is mediated by early damage of mitochondrial functions. Evidence for the involvement of mitochondrial radical generation. *J Biol Chem* 267:5317–5323.
36. Hannun YA (1996) Functions of ceramide in coordinating cellular responses to stress. *Science* 274:1855–1859.
37. Rotolo JA, et al. (2005) Caspase-dependent and -independent activation of acid sphingomyelinase signaling. *J Biol Chem* 280:26425–26434.
38. Suematsu N, et al. (2003) Oxidative stress mediates tumor necrosis factor-alpha-induced mitochondrial DNA damage and dysfunction in cardiac myocytes. *Circulation* 107:1418–1423.
39. Finkel MS, et al. (1992) Negative inotropic effects of cytokines on the heart mediated by nitric oxide. *Science* 257:387–389.
40. Brooks WW, Conrad CH, Morgan JP (1995) Reperfusion induced arrhythmias following ischaemia in intact rat heart: Role of intracellular calcium. *Cardiovasc Res* 29: 536–542.
41. Kihara Y, Morgan JP (1991) Abnormal Cai2+ handling is the primary cause of mechanical alternans: Study in ferret ventricular muscles. *Am J Physiol* 261:H1746–H1755.
42. London B, et al. (2003) Calcium-dependent arrhythmias in transgenic mice with heart failure. *Am J Physiol Heart Circ Physiol* 284:H431–H441.
43. Xiao H, et al. (2008) Positive correlation of tumor necrosis factor-alpha early expression in myocardium and ventricular arrhythmias in rats with acute myocardial infarction. *Arch Med Res* 39:285–291.
44. Ruiz-Meana M, Abellán A, Miró-Casas E, Agulló E, Garcia-Dorado D (2009) Role of sarcoplasmic reticulum in mitochondrial permeability transition and cardiomyocyte death during reperfusion. *Am J Physiol Heart Circ Physiol* 297:H1281–H1289.
45. Halestrap AP (2006) Calcium, mitochondria and reperfusion injury: A pore way to die. *Biochem Soc Trans* 34:232–237.
46. Hajnóczky G, et al. (2006) Mitochondrial calcium signalling and cell death: Approaches for assessing the role of mitochondrial Ca2+ uptake in apoptosis. *Cell Calcium* 40:553–560.
47. Jacobson J, Duchen MR (2002) Mitochondrial oxidative stress and cell death in astrocytes—requirement for stored Ca2+ and sustained opening of the permeability transition pore. *J Cell Sci* 115:1175–1188.
48. Pinton P, et al. (2001) The Ca2+ concentration of the endoplasmic reticulum is a key determinant of ceramide-induced apoptosis: Significance for the molecular mechanism of Bcl-2 action. *EMBO J* 20:2690–2701.
49. Piper HM, Meuter K, Schäfer C (2003) Cellular mechanisms of ischemia-reperfusion injury. *Ann Thorac Surg* 75:S644–S648.
50. Fauconnier J, et al. (2007) Insulin potentiates TRPC3-mediated cation currents in normal but not in insulin-resistant mouse cardiomyocytes. *Cardiovasc Res* 73:376–385.